THE REACTIONS OF GALLIUM, INDIUM AND THALLIUM WITH 2-(2-PYRIDYLAZO)-1-NAPHTHOL-4-SULPHONIC ACID AND THEIR SPECTROPHOTOMETRIC DETERMINATION

Petr VOZNICA[a], Josef HAVEL and Lumír SOMMER

Department of Analytical Chemistry,
Purkyně University, 611 37 Brno

Received October 27th, 1978

The complex equilibria of gallium, indium and thallium(III) with analytically important 2-(2-pyridylazo)-1-naphthol-4-sulphonate were studied spectrophotometrically using graphical analysis of the absorbance curves and minimization procedures for the absorbance data using the SPEKTFOT program on the Tesla 200 computer. The study yielded a complete picture of the reaction mechanism of these elements with heterocyclic azodyes. Optimum conditions for the spectrophotometric determination of gallium, indium and thallium using this reagent were found.

The reactions with gallium, indium and thallium(III) are among the analytically important reactions of heterocyclic azodyes[1-3]. The colour contrast $\sum\lambda_{complex} - \sum\lambda_{ligand}$ is increased with increasing stability of the chelates formed in the order Ga < In < Tl(III). However, the molar absorption coefficients of the complexes decrease in the same order. 2-(2-Pyridylazo)-1-naphthol-4-sulphonic acid (1-PAN-4S), derived from 1-naphthol, has some advantages over normally employed classical 1-(2-pyridylazo)-2-naphthol as a metallochromic indicator and as a spectrophotometric reagent[4-6] for a number of metals in aqueous and mixed solvent media. This work deals with a detailed study of the reactions of gallium, indium and thallium(III) with 1-PAN-4S in aqueous medium and discusses the possibility of spectrophotometric determination of small concentrations of these elements.

EXPERIMENTAL AND RESULTS

Chemicals and Solutions

2-(2-Pyridylazo)-1-naphthol-4-sulphonic acid monohydrate ($C_{15}H_{11}N_3O_4S.H_2O$, m.w. 347·3): the content of active substance was found from the carbon and nitrogen contents by elemental analysis and photometric microtitration in a formate buffer (pH 3·6) and 30% (v/v) ethanol with a copper(II) nitrate solution[4,5]. An exactly weighed amount of the reagent was dissolved in 50 ml of 5% NaOH and after dissolution the solution was diluted with doubly distilled water to 500 ml. The solution is stable for at least one month. The stock reagent solutions were not

[a] Present address: Hydroprojekt, 70 100 Ostrava.

acidified because addition of HNO_3 or $HClO_4$ results in precipitation of an orange BH^+X^- precipitate ($X = ClO_4$, NO_3).

Standard 0·16437M-$Ga(ClO_4)_3$ was prepared by dissolving metallic gallium (99·999%) in conc. HCl, the solution was repeatedly evaporated to the appearance of fumes with 70% $HClO_4$ almost to dryness and finally diluted with 0·2M-$HClO_4$. It was then standardized by EDTA titration using pyrocatechol violet.

The standard 0·10534M solution of $In(ClO_4)_3$ in 0·2M-$HClO_4$ was prepared in an analogous manner and standardized by EDTA titration using pyrocatechol violet and 1-(2-pyridylazo)-2-naphthol (ref.[21]).

Standard solution of 0·07943M-$Tl(ClO_4)_3$ in 0·45M-$HClO_4$: an alkaline solution of thallium(I) sulphate was oxidized with 30% H_2O_2; The $Tl(OH)_3$ produced was filtered off and dissolved with heating in 70% $HClO_4$. After dilution the solution was filtered and diluted to a constant volume with water. The solution was standardized chelometrically using 1-(2-pyridylazo)-2-naphthol in a chloroacetate buffer medium[20]. The content of free acid was found potentiometrically by titration with 0·1M-NaOH with evaluation of the equivalence point by Gran linearization of the titration curves.

Buffers: 1M acetate buffer (pH 4·64), 1M aminoacetate buffer (pH 2·41), 1M chloroacetate buffer (pH 2·51), 1M formate buffer (pH 3·64). The concentration given is related to the overall concentration of acid and its conjugate base. All chemicals used were of *p.a.* purity or were repeatedly recrystallized or purified in some other manner. Nitrogen oxides were removed from concentrated HNO_3 solutions by bubbling with argon or nitrogen.

Instruments

SFD-2, Unicam SP-500 or SP-700 spectrophotometers; their absorbance scales were calibrated using grey filters, the wavelength scales using 0·1M-$PrCl_3$ (444·2 nm) and $NdCl_3$ (521·6 nm, 575·5 nm). The absorbance curves of stable solutions of the reagent and its chelates with Ga(III) and In(III) were measured on a simple apparatus as described in the literature[7-9]. The solution prepared in the titration vessel was generally transferred to 1 cm cuvettes and back using a hypodermic syringe and a system of capillaries, connected by ball ground-glass joints and connected by a ground-glass joint to the cuvette. The solutions were mixed in the titration vessel in such a manner that the concentrations of the components and the ionic strength of the solution did not change. Alkaline and acidic solutions of the reagent with identical concentrations and ionic strengths were mixed in a titration vessel with several necks; in every the case the reagent solution, metal cation and electrolyte for adjusting the ionic strength of the solution, all in triple concentration, and 0·1M or 1M-NaOH were added from a burette to a solution containing all the components with the required composition at a pH value at which the reaction does not occur. If an additional component was to be added (30% ethanol), then the concentration of this component was four times that of the corresponding component in the titration vessel. In the Tl(III)–1-PAN-4S system the solutions were mixed in volumetric flasks and the absorbance was measured within 10 min. In all the measurements the initial solutions were acidic and were carefully alkalized with mixing by addition of dilute NaOH in the presence of the reagent, provided no apparent hydrolysis occurred.

Radiometer PHM 4d and PHM 64 meters with glass electrode G 202B and a saturated calomel electrode (S.C.E.) were employed. The pH meter was calibrated using aqueous NBS buffer solutions: phosphate (pH 6·48 ± 0·02; 7·00 ± 0·01), phthalate (pH 4·01 ± 0·01) and borate (9·18 ± 0·02) at 25°C.

In study of the Tl(III) and In(III) systems a capillary connector with limited diffusion, consisting of a glass tube with an S4 frit filled with 5M-$NaNO_3$ was employed to prevent contamina-

TABLE I

Survey of the Types of Transformations Used

I a single complexing reaction predominates in the whole range of analyzed experimental data, then *A*-transformations are most suitable; c_i/A-transformations are suitable when two complexing reactions partially overlap. The equilibrium constants follow from the logarithmic transformation for *y* (left-hand side of the equation) = 0.

Equilibrium		Transformation	
		$c_M = 0$	
$LH_i(\varepsilon_1) \rightleftharpoons LH_{i-1}(\varepsilon_2) + H^+;\ K_{ai}$	(*A*)	$A = \varepsilon_1 c_L + K_{ai}(\varepsilon_2 c_L - A)/[H]^+$	(*1*)
		$A = \varepsilon_2 c_L + [H](_1 c_L - A)/K_{ai}$	(*2*)
		$\log \dfrac{A - \varepsilon_1 c_L}{\varepsilon_2 c_L - A} = pH - pK_{ai}$	(*3*)
		$c_M > c_L$	
$m\,M + LH_i \rightleftharpoons M_m LH_z(\varepsilon_k) + q\,H^+\ {}^*\beta$	(*B*)	$A = \varepsilon_k c_L - \dfrac{\Delta A Z_H [H]^q Z_{OH}}{{}^*\beta c_M^m}$	(*4*)
$LH_i \rightleftharpoons LH_{i-1} + H^+;\ K_{ai}$	(*A*)	$c_L/A = 1/\varepsilon_k + \dfrac{\Delta A Z_H Z_{OH}[H]^q}{{}^*\beta c_M^m \varepsilon_k A}$	(*5*)
$M + j\,H_2O \rightleftharpoons M(OH)_j + j\,H^+;\ {}^*\beta_j$	(*C*)	$Z_{OH} = 1 + -\sum {}^*\beta_j/[H]^j$	(*6*)
		$Z_H = 1 + K_a/[H]\ \ H_2L^+$ reacting	(*7*)
		$\Delta A = A - A_L$	
		$\log \dfrac{\Delta A Z_H Z_{OH}}{\varepsilon_k c_L - A} = g\,pH + m \log c_M + \log {}^*\beta$	(*8*)
$M + LH_i \rightleftharpoons MLH_z + q\,H^+;\ {}^*\beta$	(*D*)	$c_M = c_L$	
$LH_i \rightleftharpoons LH_{i-1} + H^+;\ K_{ai}$	(*A*)	$c_L/\Delta A = 1/\varepsilon_k + \dfrac{\sqrt{\Delta A Z_H Z_{OH}[H]^q}}{A\sqrt{(c_L)\,\varepsilon_k}} \sqrt{\dfrac{\varepsilon_k c_L - A_L}{{}^*\beta}}$	(*9*)
$M + j\,H_2O \rightleftharpoons M(OH)_j + j\,H^+;\ {}^*\beta_{OH}$	(*C*)	$\log \dfrac{\Delta A Z_H Z_{OH}(\varepsilon_k c_L - A_L)}{(\varepsilon_k c_L - A)^2} = q\,pH + \log c_L + \log {}^*\beta$	(*10*)

$c_L \gtrsim c_M$

$$c_M/\Delta A = 1/(\varepsilon_k - nA_L/c_L) + \frac{Z^n\,[H]^q}{(c_L - n\,\Delta A/(\varepsilon_k - nA_L/c_L))^n(\varepsilon_k - nA_L/c_L)\,{}^*\beta} \quad (11)$$

$c_L > c_M$

$M + n\,LH_i \rightleftharpoons ML_nH_z(\varepsilon_k) + q\,H^+;\ {}^*\beta$ (E)

$$c_M/\Delta A = 1/\varepsilon_k + \frac{Z_H^n Z_{OH}\,[H]^q}{\varepsilon_k c_L^n\,{}^*\beta} \quad (12)$$

$LH_i \rightleftharpoons LH_{i-1} + H^+;\ K_{ai}$ (A)

$$\Delta A = \varepsilon_k c_M - \Delta A\,[H]^q\,Z_H^n Z_{OH}/c_L^n\,{}^*\beta \quad (13)$$

$M + j\,H_2O \rightleftharpoons M(OH)_j + H^+;\ {}^*\beta_{OH}$ (C)

$$\log \frac{\Delta A Z_H^n Z_{OH}}{\varepsilon_k c_M - \Delta A} = q\,pH + n \log c_L + \log {}^*\beta \quad (14)$$

$\Delta A = A - A_L$

$c_L > c_M$

$MLH_z(\varepsilon_1) + LH_2 \rightleftharpoons ML_2H_s(\varepsilon_2) + q\,H^+\ {}^*K_2$ (F)

$$\Delta A = \varepsilon_2 c_M - \frac{(\Delta A - \varepsilon_1 c_M)\,Z_H\,[H]^q}{{}^*K_2 c_L} \quad (15)$$

$$\Delta A = \varepsilon_1 c_M + \frac{(\varepsilon_2 c_M - \Delta A)\,{}^*K_2 c_L}{z_H\,[H]^q} \quad (16)$$

$$\log \frac{\Delta A - \varepsilon_1 c_M}{\varepsilon_2 c_M - \Delta A} Z = q\,pH + \log c_L + \log {}^*K_2 \quad (17)$$

$c_L > c_M$

$MLH_z + H_2O \rightleftharpoons MLH_s(OH) + q\,H^+\ {}^*K_{OH}$ (G)

Relationships analogous to (16) and (17) except $c_L = 1$, $Z_H = 1$

$c_L > c_M$

$M + LH_2 \rightleftharpoons ML(\varepsilon_1) + 2\,H^+\ {}^*\beta_1$ (I)

$\Delta A = \varepsilon_2 c_M + (\varepsilon_1 c_M - \alpha\,\Delta A)\,[H]/{}^*K_2$ (18)

$ML + H_2O \rightleftharpoons ML(OH)\,(\varepsilon_2) + H^+;\ {}^*K_2$ (J)

$\alpha\,\Delta A = \varepsilon_1 c_M + (\varepsilon_2 c_M - \Delta A)\,{}^*K_2/[H^+]$ (19)

$ML + H_2L \rightleftharpoons ML_2H_z(\varepsilon_2) + q\,H^+;\ {}^*K_2$ (L)

$\alpha\,\Delta A = \varepsilon_1 c_M + {}^*K_2(\varepsilon_2 c_M - \Delta A)\,c_L/[H^+]$ (20)

$LH_2 \rightleftharpoons LH + H^+;\ K_{a1}$ (A)

(simultaneous formation of equilibria (I) and (J) or (I) and (L)

$\alpha = 1 + [H]^2\,Z_H/{}^*\beta_1 c_L$ (21)

${}^*K_1$, must be known beforehand

$$\log \frac{\alpha\,\Delta A - \varepsilon_1 c_M}{\varepsilon_2 c_M - \Delta A} = pH + \log {}^*K_2 \quad (22)$$

Collection Czechoslov. Chem. Commun. [Vol. 45] [1980]

tion of solutions by Cl^- ions from the S.C.E. and for solutions with pH > 1 and $I = 0{\cdot}1$. At this electrolyte concentration the system exhibited minimal deviations from the theoretical dependence, $E = f(\mathrm{pH})$. For measurements at higher acidities a capillary connection with free diffusion and a concentrated $NaNO_3$ solution were employed. The calibration of the glass electrode against the S.C.E. was then carried out using solutions with known acid concentrations and constant anion concentrations (I 2M) or by mixing equimolar solutions of $NaClO_4 + HClO_4$ or $HNO_3 + NaNO_3$. The $E = f(-\log [H])$ dependence is linear over the range $-\log [H] = -0{\cdot}3$ to $1{\cdot}0$; from $-\log c_H - 0{\cdot}3$ this dependence becomes nonlinear. This method of measurement is also useful for mixed media containing ethanol.

Method of Studies

In the study of chemical equilibria in solutions and to determine the optimum conditions for the spectrophotometric determination of these elements, the already tested combination of graphical and graphical logarithmic analysis of absorbance curves and treatment of spectrophotometric data using a computer was employed (*e.g.*[5,7,15]). Absorbance curves of solutions with an excess of one component or equimolar solutions in dependence on the pH or on the concentration of the reacting component were interpreted using slope-intercept transformations of the equilibrium constants or conditional stability constants of the assumed chelate for conditions under which a single complex equilibrium predominates and for chosen wavelengths[10]. A summary of the types of transformations employed is given in Table I. Data for a greater number of wavelengths for selected absorbance curves were treated by linear regression of the linear transformations numerically using the PRCEK T 200 program[5,11–13]. The SPEFO 8 program, an extended version of the SPEKTFOT 4 program (ref.[5,14,15]), was employed for interpretation of overlapping complex equilibria and in the presence of a greater number of absorbing species in solution. This program is extended by additional parameters which, although they cannot be minimized simultaneously, permit inclusion of additional equilibria in the calculation. In the expression

$$U = \sum_{i=1}^{N} W_i (A_{exp} - A_{calc})^2 = \text{minimum} \qquad (23)$$

the statistical weights are $W_i = 1$ for all the experimental points. The calculated absorbance values A_{calc} are given by the relationship

$$A_{calc} = \sum_{i=1}^{N_k} \varepsilon_i [M_m L_n H_x] , \qquad (24)$$

where $M_m L_n H_x$ designates the equilibrium concentration of all the absorbing species in solution. With choice of a suitable model, *i.e.* with choice of the most probable composition of the complex formed, a procedure was followed whereby the given complex was considered valid if its introduction into the model or set of species led to minimization that resulted in a decrease in the U value and if the standard deviation values were satisfactory, *i.e.* $\beta_i > F_s s_{(\beta i)}$, where $s_{(\beta i)}$ is the standard deviation of β_i and rejection factor $F_s = \beta_i / s_{(\beta i)} = 2$ corresponds to significance level $\alpha = 0{\cdot}977$, *i.e.* calculated constant β_i is valid with 99·7% probability in the interval $\beta_i \pm s_{(\beta i)}$. The initial data were calculated from graphical analysis of the absorbance-pH curves. With suitably chosen minimization procedures the individual parameter steps were $0{\cdot}1$ for $\log \beta_i$ and 500 for ε.

Acid-Base Properties of 1-PAN-4S

The pK_{ai} values and the molar absorption coefficients found graphically and by calculation using the PRCEK and SPEKTFOT programs from absorbance-pH curves of the reagent for aqueous media are given in Tables II and III.

Graphical Analysis of Absorbance Curves of Ga, In, Tl(III) *and* 1-PAN-4S *Solutions*

In solutions with excess Ga^{3+} [c_M/c_L = 20, 100, $c_L = 2{\cdot}0 \,.\, 10^{-5}$M, I = 0·1 and 20, 100, 200 (I = 1·0, KNO_3)] and for 540 nm, transformations (*4*), (*5*) and (*8*) of the absorbance-pH curves indicated unambiguously the presence of equilibria (K) and (L)

$$Ga^{3+} + H_2L^+ \rightleftharpoons GaL + 2\,H^+ \qquad (K);\ {}^*\beta_{1(2)}$$

$$Ga^{3+} + HL \rightleftharpoons GaL + H^+ \qquad (L);\ {}^*\beta_{1(1)}$$

over the entire formation interval pH 1·5–3·0 (Fig. 1). Consideration of simultaneous hydrolysis, $Ga^{3+} \rightarrow Ga(OH)_i$ (i = 1, 2, 3) with ${}^*K_1 = 1{\cdot}35 \,.\, 10^{-3}$, ${}^*K_2 = 2{\cdot}1 \,.\, 10^{-4}$, ${}^*K_3 = 3{\cdot}0 \,.\, 10^{-5}$ (ref.[16]) (Table I, Eq. (*6*)), has no important effect on the course of transformations (*4*) and (*5*) in the given pH interval. These results are confirmed by the $A = f(c_M)$ analysis in solutions with excess c_M at pH 2·30 and 2·50 and at constant concentration $c_L = 5{\cdot}0 \,.\, 10^{-5}$M according to transformation (*5*). They also follow from the constant values of the equilibrium constants $\log {}^*\beta_1$ from equation (*8*) at various pH values. The formation of GaL (λ_{max} 312 nm, ε 1·10 . 10^4; λ_{max} 377 nm, ε 1·08 . 10^4; λ_{max} 524 nm, ε 2·08 . 10^4) from the reagent in

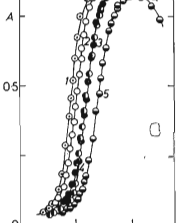

FIG. 1

Absorbance-pH Curves for Solutions of 1-PAN-4S with Excess Ga^{3+}

c_L M 2·0 . 10^{-5}M, 540 nm, l 2 cm, c_M/c_L, I: Curve *1* 200, 1·0; *2* 100, 0·1 and 1·0; *3* 20, 0·1; *4* 20, 1·0; *5* $c_M = c_L = 4{\cdot}0 \,.\, 10^{-5}$M, l 1 cm.

the H_2L^+ form (λ_{max} 362, 459 nm) is characterized on the absorbance curves in dependence on the pH by sharp isosbestic points at 334, 388, 402 and 482 nm (Fig. 2). For most of the absorbance-pH curves (pH 2·0—2·7) for equimolar solutions (curve *5* on Fig. 1), transformations (*9*) and (*10*) confirmed the existence of the 1 : 1 chelate in the sense of equilibrium (K). The absorbance curves exhibit the same maxima as observed for solutions with excess metal cations, but only two isosbestic points at

TABLE II
Dissociation Constants of 1-PAN-4S in Aqueous Media

$pK_{a1}(\pm 3s_{pK})$	$pK_{a2}(\pm 3s_{pK})$	I
2·89[a]	7·75[a]; 7·79[a]	1·0(KNO_3)
2·873 ± 0·027[b]	7·889 ± 0·015[e]	1·0(KNO_3)
2·874 ± 0·009[c]		1·0(KNO_3)
2·879 ± 0·030[d]	7·888 ± 0·020[b]	0·1(KNO_3)

[a] Graphical logarithmic analysis for 520 and 540 nm; [b] direct graphical analysis with the PRCEK T 200 program (average of values for 8 wavelenghts); [c] logarithmic analysis with the PRCEK T 200 program (average of values for 8 wavelengths); [d] SPEKTFOT 4 program, [d] average of values for 4 wavelengths; [e] average for 8 wavelengths; [f] average for 4 wavelengths.

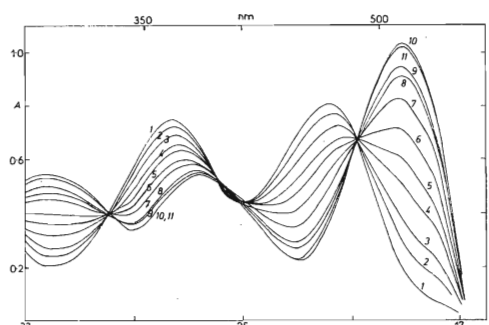

FIG. 2
Absorbance Curves for Solutions of 1-PAN-4S with Excess Ga^{3+}; $c_M = 2·5 \cdot 10^{-3}$M, $c_L = 5·0 \cdot 10^{-5}$M, I 0·1
pH: Curve *1* 0·99; *2* 1·23; *3* 1·35; *4* 1·45; *5* 1·56; *6* 1·67; *7* 1·76; *8* 1·84; *9* 1·96; *10* 2·24; *11* 2·41.

TABLE III

Molar Absorption Coefficients of Various Acido-Basic Forms of 1-PAN-4S at Various Wavelengths

370	380	500	520	530	540	550	560
			$\varepsilon \cdot \text{mol}^{-1}\,\text{l} \cdot \text{cm}^{-1}$				
			H_2L^*				
16 569 ± 55[a]	14 439 ± 45	10 571 ± 69	4 691 ± 52	2 656 ± 28	1 349 ± 25	657 ± 5	387 ± 25
16 685 ± 90[b]	14 495 ± 72	10 527 ± 108	4 689 ± 81	16 625[c]	1 762 [d]		
			HL^-				
11 943 ± 15[a]	9 350 ± 24	18 209 ± 21	11 439 ± 21	7 285 ± 25	3 884 ± 6	1 953 ± 3	1 128 ± 6
11 935 ± 48[b]	9 359 ± 57	18 184 ± 90	11 447 ± 44	8 644 ± 63	3 964 ± 50	2 016 ± 30	1 183 ± 30
11 946 ± 36[b]	9 371 ± 32	18 139 ± 28	11 452 ± 66	12 500[e]	20 375[f]		
			L^{2-}				
3 854 ± 33	2 915 ± 29	21 947 ± 26	17 470 ± 57	13 983 ± 72	9 838 ± 43	5 831 ± 48	3 118 ± 25
			17 512 ± 45		9 582 ± 44	5 885 ± 5	3 078 ± 17

[a] PRCEK program, [b] SPEKTFOT 4 program for I 0·1 and 1·0, [c] graphically for λ_{max} 365 nm, [d] λ_{max} 463 nm, [e] λ_{max} 358 nm, [f] λ_{max} 480 nm, remaining values from absorbance-pH curves or transformations (*1*) and (*2*).

336 and 478 nm. Equilibrium (E) was tested primarily in solutions with excess ligand, ($c_M = 2{\cdot}0 \,.\, 10^{-5}$M, $c_L/c_M = 7{\cdot}5$, 15, 20) (Fig. 3) using equations (*11*)–(*14*) and also equilibria with complex transformations (F) and (G) with transformations (*15*) and (*16*). For $c_L/c_M = 7{\cdot}5$ and pH 1·5–3·0 none of these transformations was linear for the assumed actual number of split protons. Transformations (*18*) and (*19*) were linear for the final part of the pH curve above pH 3·0, assuming simultaneous reactions

$$Ga + H_2L \rightleftharpoons ML + 2\,H^+ \qquad (K)\ {}^*\beta_{1(2)}$$

$$GaL + H_2O \rightleftharpoons GaL(OH) + H^+ \qquad (L)\ {}^*K_{OH1}$$

after substitution of equilibrium constants ${}^*\beta_1$ (Table V) into the relationship. For absorbance-pH curves for solutions with $c_L/c_M = 15$ and 20, transformations (*12*) and (*14*) prove two different complex formation regions. At pH 1·8–2·5 or pH 2·0 to 2·7, equilibrium K is predominant with extrapolated value $\varepsilon = (2{\cdot}22-2{\cdot}27) \,.\, 10^4$ at 540 nm, equal to the value for equimolar solutions and solutions with excess Ga^{3+}. In the pH region 3·0–4·0 or 2·7–3·1 and with final value $\varepsilon = (2{\cdot}90-3{\cdot}20) \,.\, 10^4$ at 540 nm, transformations (*15*)–(*17*) indicated the splitting of a single proton for complex transition according to probable equilibria (K), (L) or (M)

$$GaL + H_2L \rightleftharpoons GaL(LH) + H^+ \qquad (M)\ {}^*K_2.$$

If the limiting value $\varepsilon_k = (2{\cdot}90-3{\cdot}20) \,.\, 10^4$ from (*12*) and (*13*) for 540 nm is employed in logarithmic transformation (*8*), a marked linear portion appears with slope $q = 2{\cdot}0$ at pH $\leqq$ 2·6 and another with slope $q = 2{\cdot}85-3{\cdot}00$ for pH 2·7–3·9 ($c_L/c_M = 15$)

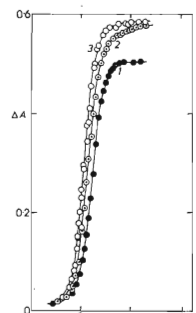

FIG. 3

Absorbance-pH Curves for Ga^{3+} Solutions with Excess 1-PAN-4S

540 nm, $c_M = 2{\cdot}0 \,.\, 10^{-5}$M, $A = A - A_L$, c_L/c_M: Curve *1* 7·5; *2* 15; *3* 20.

and pH 2·7–3·1 ($c_L/c_M = 20$), corresponding to collective splitting of protons in the two equilibria (K) and (L) or (M). The complex with component ratio Ga : L = = 1 : 2 was also not indicated on the absorbance dependence $A = f(c_L)$ at pH < 4. At pH > 4, the complex with Ga^{3+} is only slightly dissociated; the dependences have the character of molar ratio curves and again indicate a Ga : L ratio of 1 : 1. The continuous variation curves, $Y = A - A_L = f(x_L)$ for $c_0 = (3{\cdot}0-4{\cdot}0) \cdot 10^{-5}$M have a maximum for $x_L = 0{\cdot}53-0{\cdot}60$ at 540 nm. The small shift of the maximum from a ratio of M : L = 1 : 1 to higher x_L values which is identical for various wavelengths or pH values employed, need not be only the indication of a small amount of a complex with M : L = 1 : 2 but even the consequence of a oligonuclear hydrolysis of Ga^{3+}.[24] The differential absorption curves of solutions of mixtures of complexes have λ_{max} 548 nm ($\varepsilon = 2{\cdot}70 \cdot 10^4$) at pH 3·70, where the reagent and complex solutions were measured against water. Dimer formation was not probable in solutions exhibiting marked hydrolysis of Ga^{3+} considering equilibria (N) and

TABLE IV

Molar Absorption Coefficients from Graphical Analysis of the Absorbance Curves (540 nm)

Complex	$\varepsilon \cdot 10^{-4}$, $mol^{-1}\,l \cdot cm^{-1}$
GaL	2·22[a]; 2·16[b]; 2·07[c]; 2·17[d]; 2·27[e]
GaL(OH)	2·86[f]; 2·93[g]; 2·53[b]; 2·90[b]; 2·89–3·20[e]
InL	2·50[a]; 2·55[b]; 2·44[c]; 2·50[d]; 2·58[e]; 2·54; 2·50; 2·17[f]; 2·40[e,f]; 2·50[g]
InL_2	3·48[d]; 3·41[d,f]; 3·45; 3·50[g]
TlL	2·05[a,b]; 2·05[d]; 1·94[e]
TlL_2	3·48[b]; 3·35[c]; 3·40[e]

[a] $c_M/c_L = 100, 10$; [b] $c_M = c_L$; [c] $c_L/c_M = 10$, $c_M = 8{\cdot}0 \cdot 10^{-6}$M; [d] $c_L/c_M = 10$; $c_M = 2{\cdot}0 \cdot 10^{-5}$M; [e] pH 1·9 or 2·2 ($A = f(c_M)$); [f] from the plateuax, $A = f$(pH); [g] $c_L/c_M = 20$, $c_M = 2{\cdot}0 \cdot 10^{-5}$M.

[a] $c_M/c_L = 10$($I = 2{\cdot}0$; ClO_4^-; NO_3^-); [b] $c_L/c_M = 10$($I = 2{\cdot}0$, NO_3^-); [c] from the plateaux $A = = f$(pH) for $c_L/c_M = 10$; [d] $c_M/c_L = 10$(I 0·1, NO_3^-); [e] $c_L/c_M = 18{\cdot}6$(I 2·0; NO_3^-).

(*O*), as transformations for these solutions indicated a lower number of split protons than that following from the assumed equilibria

$$2\,ML + 2\,H_2O \rightleftharpoons ML(OH)_2ML + 2\,H^+ \qquad (N)$$

$$2\,M + 2\,H_2L + 2\,H_2O \rightleftharpoons ML(OH)_2ML + 6\,H^+ . \qquad (O)$$

The values of the molar absorption coefficients found and the calculated equilibrium constants are given in Tables IV and V.

Graphical analysis of the pH-absorbance curves of solutions with excess indium ($c_L = 2{\cdot}0 \cdot 10^{-5}$M, $c_M/c_L = 10$, 100, *I* 0·1) using transformation (*5*) indicated the

TABLE V

Equilibrium Constants Obtained from Graphical Analysis of the Absorbance Curves (540 nm, *I* 0·1)

Equilibrium	log *K*
$*\beta_1(Ga^{3+} + H_2L \rightleftharpoons GaL + 2\,H)$	−1·30; −1·40(*I* 1·0); −1·34; −1·40[a], −1·36[b]; −1·00[g]; −0·70[f]; −0·58[e]; −0·76[h]; −1·24[c]; −1·27[d]

[a] From absorbance-pH curves, $> c_M$, $c_M = c_L$, $> c_L$; [b] $c_M = c_L$; [c] at pH 2·3, $> c_M$; [d] at pH 2·5, $> c_M$; [e] from pH curves, $c_L/c_M = 20$; [f] $c_L/c_M = 15$; [g] $c_L = c_M$; [h] $c_M/c_L = 15$ (*I* 0·1), correction for hydrolysis.

$*\beta_1(In^{3+} + H_2L \rightleftharpoons InL + 2\,H^+)$	−1·00[a]; −1·10[a]; −0·76[b]; M0·89[c]; −1·05[c]; −0·40[d]
$K_2(InL + H_2L \rightleftharpoons InL_2 + 2\,H^+)$	−2·86[e]; −2·26[d]

[a] $c_M/c_L = 10$, 100; [b] $c_M = c_L$; [c] pH 1·9 and 2·2, $A = f(c_M)$; [d] $c_L/c_M = 20$, $c_M = 2{\cdot}0 \cdot 10^{-5}$M; [e] $c_L/c_M = 10$, $c_M = 2{\cdot}0 \cdot 10^{-5}$ *B*

$*\beta_1(Tl^{3+} + H_2L \rightleftharpoons TlL + 2\,H^+)$	3·6[a]; 3·5[b]; 3·7[c]
$K_2(TlL + H_2L \rightleftharpoons TlL_2 + 2\,H^+)$	1·7[b]; 1·8[c]

[a] $c_M/c_L = 10$(*I* 2·0; ClO_4^-, NO_3^-); [b] $c_L/c_M = 10$(*I* 2·0; NO_3^-); [c] $c_L/c_M = 18{\cdot}6$ (*I* 2·0; NO_3^-); in solutions with excess c_M corrections for the hydrolysis $Tl(III) \rightarrow Tl(OH)_i^{3-i}$ were employed.

presence of equilibria (P) and (R)

$$In^{3+} + H_2L^+ \rightleftharpoons InL + 2\,H^+ \qquad (P)\ {}^*\beta_{1(2)}$$

$$In^{3+} + HL \rightleftharpoons InL + H^+ \qquad (R)\ {}^*\beta_{1(1)}$$

at pH < 3. These equilibria were also confirmed by analysis of the concentration dependence $A = f(c_M)$ for solutions with excess metal cation and $c_L = 5{\cdot}0 \,.\, 10^{-5}$M at pH 1·90 or 2·20 according to (*5*) and also recalculation of the conditional stability constants for the InL chelate to equilibrium constants in the sense of equilibrium (P) according to (*8*). Analysis of equimolar absorbance pH curves also gives analogous results ($c_L = c_M = 5{\cdot}0 \,.\, 10^{-5}$M) according to relationships (*9*) and (*10*). The extrapolated values of the molar absorption coefficients are practically identical for all cases (Table IV) (Fig. 4). Two sections are visible on the absorption-pH curves of solutions with excess ligand, at pH 1·5–2·5 and at pH 2·7–4·0, within which two different equilibria are established (Fig. 5). Equilibrium (P) was shown to be present in solutions with $c_L/c_M = 10$ and $c_M = 2{\cdot}0 \,.\, 10^{-5}$M at pH 1·50–2·70 using transformations (*12*) and (*14*) with extrapolated value $\varepsilon_k = 2{\cdot}50 \,.\, 10^4$. The remaining part

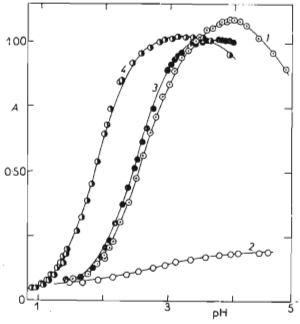

FIG. 4

Absorbance-pH Curves for 1-PAN-4S Solutions with Excess In^{3+}

$c_L = 2{\cdot}0 \,.\, 10^{-5}$M, 540 nm; *I* 0·1; c_M/c_L: Curve *1* 100; *2* 10; *3* 1; *4* reagent alone.

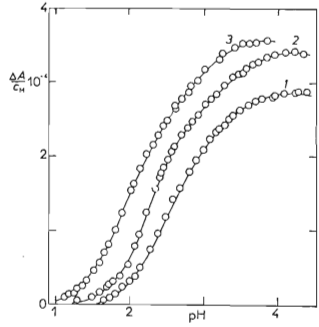

FIG. 5

Absorbance-pH Curves for In^{3+} Solutions with Excess 1-PAN-4S; $A \,.\, 10^{-4}/c_M$; 540 nm, *I* 0·1

Curve *1* $c_L = 8{\cdot}0 \,.\, 10^{-5}$M; $c_M = 8{\cdot}0 \,.\, 10^{-6}$M; *2* $c_L = 2{\cdot}0 \,.\, 10^{-4}$M, $c_M = 2{\cdot}0 \,.\, 10^{-5}$M, *3* $c_M = 2{\cdot}0 \,.\, 10^{-5}$M, $c_L = 4{\cdot}0 \,.\, 10^{-4}$M.

of the pH curve at pH 2·7 could be extrapolated to $\varepsilon_k = 3{\cdot}48 \cdot 10^4$. With the two values of the molar absorption coefficient, single equilibrium (S) of the two possible complex transformations (F) and (G) at pH 3·0–4·1 after multiple approximations to the shape of transformations (15)–(17) was obtained:

$$InL + H_2L \rightleftharpoons InL_2 + 2\,H^+ . \qquad (S)\ {}^*K_2$$

Analogous conditions exist in solutions with $c_L/c_M = 10$ ($c_M = 8{\cdot}0 \cdot 10^{-6}$M), except that less complex InL_2 is formed and equilibria (P) and (S) overlap more. In solutions with $c_L/c_M = 20$ ($c_M = 2{\cdot}0 \cdot 10^{-5}$M), equilibrium (S) predominates at pH 2·5–3·2; in solutions with a ratio of $c_L/c_M = 7{\cdot}5$, transformations (18), (20)–(22) indicated that conditions in the cell were favourable for formation of a mixture of complexes InL and InL_2. Interpretation of curves $A = f(c_L)$ according to (12) and (13) indicated a mixture of complexes with M : L = 1 : 1 and 1 : 2 at pH < 4. At pH ≧ 4·2 these dependences have the character of molar ratio curves and indicate the stoichiometric composition of the complex, In : L = 1 : 2. Job plots ($c_0 \sim 10^{-5}$M) indicate shift of the maximum from $x_L = 0{\cdot}5$ at pH 3·0 to $x_L = 0{\cdot}60$ at pH 3·95, *i.e.* again a mixture of complexes with In : L = 1 : 1 and 1 : 2. The curve maximum is not affected by the wavelength in the range 450–500 nm. At pH > 4·0 a precipitate is formed as a result of hydrolysis of the complex and the theoretical position of the maximum for $x_L = 0{\cdot}67$ cannot be confirmed. In solutions with excess cation and in equimolar solutions the absorption spectra correspond to the InL complex (λ_{max} = 530–532 nm, $\varepsilon = (2{\cdot}10-2{\cdot}35) \cdot 10^4$) and transition from H_2L^+ (λ_{max} = 467–465 nm) to InL is characterized by an isosbestic point at 487–494 nm. In solutions with excess ligand the differential spectra of the InL_2 complex have λ_{max} 558 nm ($\varepsilon = 3{\cdot}23 \cdot 10^4$) if the curve is measured point by point, *i.e.* the solution of the complex with excess reagent against water and the reagent against water as a blank. The values of the molar absorption coefficient for the individual complexes and the equilibrium constants are summarized in Tables IV and V.

The formation curves for the complex of 1-PAN-4S with Tl(III) are shifted markedly to more acid media in solutions with excess metal cation. Analysis of the absorbance-pH curves of solutions with $c_M/c_L = 10{\cdot}75$ ($c_L = 4{\cdot}0 \cdot 10^{-5}$M, I 2·0 (KNO_3)) using transformations (4), (5) and (8) and for $-\log c_H = -0{\cdot}3$ to 0·7 indicates formation of TlL according to equation (T):

$$Tl^{3+} + H_2L^+ \rightleftharpoons TlL^{2+} + 2\,H^+ , \qquad {}^*\beta_{1(2)}\ (T)$$

curve 2 in Fig. 6). In the presence of ClO_4^- (I 2·0) the absorbance-pH curve is deformed (curve 3 in Fig. 6), probably as a result of the formation of ion associates $TlL^{2+}.2\,ClO_4^-$. In analysis of absorbance curves of solutions with excess reagent ($c_L/c_M = 9{\cdot}29$, $c_M = 2{\cdot}15 \cdot 10^{-5}$M, I = 2·0 (NO_3^-)) using transformations (12)–(14), equilibrium

(T) was found to be present for $-\log c_H = -0{\cdot}3$ to $0{\cdot}5$; in the range $-\log c_H = 0{\cdot}7-1{\cdot}5$ complex transition according to equation (U) predominates

$$TlL^{2+} + H_2L^+ \rightleftharpoons TlL_2^+ + 2\,H^+ \qquad {}^*K_2\ (U)$$

as follows from stepwise approximation to dependences (*15*) and (*16*) and logarithmic transformation (*15*) (curve 2, Fig. 7). In solutions with I 0·1 (NO_3^-) the two complex equilibria (T) and (U) overlap at pH > 0·2, with the latter predominating at pH 0·4 to 1·3 with a small reagent excess (indicated using transformations (*18*) and (*20*) after substitution of equilibrium constant ${}^*\beta_1 = 10^{3.6}$ and (*22*)). In solutions with larger reagent excesses ($c_L/c_M = 18{\cdot}6$, $c_M = 1{\cdot}152 \cdot 10^{-5}$M, I 2·0 (NO_3^-)) equilibrium (T) predominates at $-\log c_H = -0{\cdot}3$ to 0·1 and transition of complex (U) predominates at $-\log c_H = 0{\cdot}7-1{\cdot}2$ (curve 3 in Fig. 7). Curves of the dependence of the absorbance on the concentration of the reagent from pH 2·02 (I 0·2) and $-\log c_H = 2{\cdot}0$, NO_3^-) have the character of molar ratio curves and indicate stoichiometric composition of the complex with Tl : L = 1 : 2. Job curves of solutions with I 2·0

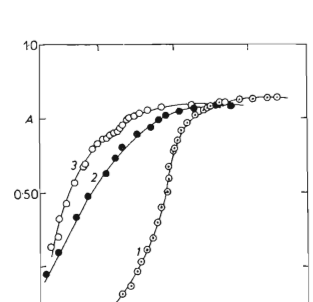

FIG. 6

Absorbance-pH Curves for 1-PAN-4S Solutions with Excess Tl^{3+}

540 nm; Curve *1* $c_M = 2{\cdot}0 \cdot 10^{-4}$M, $c_L = 2{\cdot}0 \cdot 10^{-5}$M, I 0·1; *2* $c_M = 4{\cdot}3 \cdot 10^{-4}$M, $c_L = 4{\cdot}0 \cdot 10^{-5}$M, I 2·0 (NO_3^-); *3* $c_M = 4{\cdot}3 \cdot 10^{-4}$M; $c_L = 4{\cdot}0 \cdot 10^{-5}$M, I 2·0 (ClO_4^-); *4* $c_M = 0$, $c_L = 4{\cdot}0 \cdot 10^{-5}$M, I 2·0 (NO_3^- or ClO_4^-). Curves *1*, *4*: x = pH; curves *2*, *3*: $x = -\log c_H$.

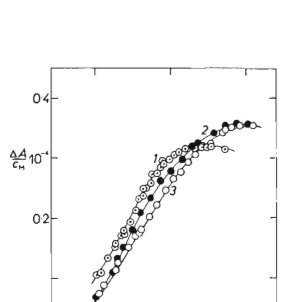

FIG. 7

Absorbance-pH Curve of Tl(III) Solutions with Excess 1-PAN-4S (A/c_M) . 10^{-4}; 540 nm

1 x = pH, $c_L = 1{\cdot}0 \cdot 10^{-4}$M, $c_M = 1 \cdot 10^{-5}$M, I 0·1, l = 2 cm; *2* $x = -\log c_H$, $c_L = 2{\cdot}0 \cdot 10^{-4}$M, $c_M = 2{\cdot}152 \cdot 10^{-5}$M; I 2·0 (NO_3^-), l 10 mm; *3* $x = -\log c_H$, $c_L = 4{\cdot}0 \cdot 10^{-4}$M, $c_M = 2{\cdot}152 \cdot 10^{-5}$M, I 2·0 (NO_3^-), l 10 mm.

(NO_3^-) ($c_0 \sim 10^{-5}$) exhibit a shift of the maximum at 540 nm from $x_L = 0{\cdot}50$ for $\log c_H = 0{\cdot}5$ to value $x_L = 0{\cdot}63$ for $-\log c_H = 2{\cdot}0$; at higher $-\log c_H$ values the solution readily hydrolyzes. This is again an indication of the presence of a mixture of complexes with Tl : L = 1 : 1 and 1 : 2 in solution. Absorbance curves of solutions with excess Tl(III) ($c_M/c_L = 10{\cdot}8$, $c_L = 4{\cdot}0 \,.\, 10^{-5}$M, I 2·0 (NO_3^-)) indicate transition of H_2L^+ (λ_{max} 369 nm, $\varepsilon = 1{\cdot}75 \,.\, 10^4$, 472 nm, $\varepsilon = 1{\cdot}93 \,.\, 10^4$) to complex TlL ($\lambda_{max}$ 388 nm, $\varepsilon = 1{\cdot}06 \,.\, 10^4$, λ_{max} 570 nm, $\varepsilon = 2{\cdot}08 \,.\, 10^4$) with an isosbestic point at 510 nm (Fig. 8). Completely analogous values resulted from a set of absorption curves for $-\log c_H = 2{\cdot}0$ and I 2·0 (NO_3^-) and $c_L = 3{\cdot}23 \,.\, 10^{-5}$M with increasing concentration of Tl^{3+}. In solutions with excess $c_L/c_M = 2{\cdot}045$ ($c_M = 3{\cdot}23 \,.\, 10^{-5}$, I 2·0) the complex has λ_{max} 382 nm ($\varepsilon = 2{\cdot}29 \,.\, 10^4$) and 565 nm ($\varepsilon = 3{\cdot}34 \,.\, 10^4$) and an isosbestic point for the transition for $-\log c_H = -0{\cdot}35$ to $+0{\cdot}35$ at 510 nm. The values of the molar absorption coefficient and equilibrium constant found from graphical analysis of the absorption curves are given in Tables IV and V.

Numerical Analysis of Absorbance Data for the 1-PAN-4S *System with* Ga^{3+}, In^{3+} *and* Tl^{3+} *Using the* SPEKTFOT *Minimization Program on the* TESLA 200 *Computer*

In Ga^{3+} solution with excess $c_M/c_L = 20$, $c_L = 2{\cdot}0 \,.\, 10^{-5}$M, in the pH region 0·66 to 3·54 at 540 nm (altogether 32 experimental points), the experimental data agree

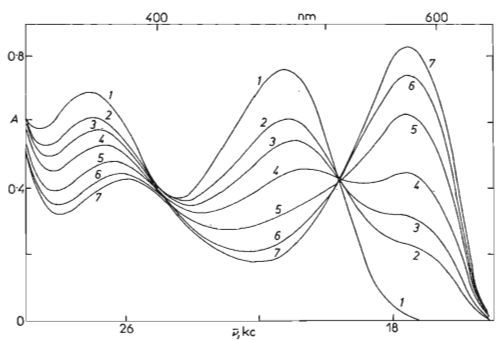

FIG. 8

Absorbance Curves for 1-PAN-4S Solutions with Excess Tl(III)

$c_M = 4{\cdot}3 \,.\, 10^{-4}$M, $c_L = 4{\cdot}0 \,.\, 10^{-5}$M, I 2·0 (NO_3^-), $-\log c_H$. Curve *1* 0·200 ($c_M = 0$); *2* —0·350; *3* —0·270; *4* —0·143; *4* 0·045; *6* 0·173; *7* 0·350.

very well with the equilibrium model for formation of chelate GaL^{2+} alone, in good agreement with the graphical analysis. The set of initial and minimized data for optimum fit is given in Table VI. For solutions with excess 1-PAN-4S the experimental data was treated for 540 nm, $c_L/c_M = 20$ ($c_M = 2{\cdot}00 \cdot 10^{-5}$M at pH 1·50–3·30 (altogether 19 experimental points) and for $c_L/c_M = 15$, $c_M = 2{\cdot}00 \cdot 10^{-5}$M, pH 2·00 to 4·40 (altogether 25 experimental points). Considering the results of graphical analysis of the absorption curves, various combinations of possible species were considered in the minimization program, *i.e.* GaL, GaL(OH), GaL_2H and GaL_2, simultaneously with the products of hydrolysis of Ga^{3+}, Ga(OH) and $Ga(OH)_2$. Extensive minimization procedures for all possible binary and ternary models indicated that the most probable model is model 5 (Table VII), which, under the experimental conditions, considers simultaneous presence of GaL, GaL_2H and GaL(OH) in solutions with excess PANS ($c_L = 3{\cdot}00 \cdot 10^{-4}$M and $4{\cdot}00 \cdot 10^{-4}$M) at pH 1·40–4·40, with simultaneous hydrolysis of Ga^{3+} to $GaOH^{2+}$ and $Ga(OH)_2^+$. The model gives a good fit for curves for solutions with excess reagent and the best constant agreement for both reagent concentrations and the corresponding sequence and ratios of the molar absorption coefficients for the individual complexes. Only for GaL(OH) is the difference in ε for the two series of experimental data rather different. It follows, however, from the distribution diagrams that, in solutions with $c_L = 4{\cdot}00 \cdot 10^{-4}$M, the GaL(LH) complex is formed to only a slight degree (<15%), leading to a greater error in the calculated values of the molar absorption coefficient.

The assumption of a mixture of GaL and GaL(OH) in addition to hydrolysis of Ga^{3+} to the hydroxo complexes (model 1) follows from the conclusions of graphical analysis and, although it gives good fit for the absorbance curves, the resulting values

TABLE VI

Analysis of the Absorbance-pH Curves by the SPEKTFOT Program ($c_L = 2{\cdot}0 \cdot 10^{-5}$M, $c_M/c_L = 20$, I 0·1, 540 nm; Ga^{3+} — 1-PANS, excess metal).

Complex	log β	$\varepsilon + \Delta\varepsilon$	U	σ, A
GaL	9·398 ± 0·007	21 995 ± 79	$3{\cdot}931 \cdot 10^{-4}$	±0·0036

Data from graphical analysis (input estimates):

$pK_{a1}(LH_2 \rightleftharpoons LH + H^+) = 2{\cdot}89$
$pK_{a2}(LH \rightleftharpoons L + H^+) = 7{\cdot}79$
$\log \beta_1(Ga + L \rightleftharpoons GaL) = 9{\cdot}44$
$\varepsilon_1(GaL) = 21\,500$

$\varepsilon(LH_2) = 1\,240$
$\varepsilon(LH) = 3\,900$
$\varepsilon(L) = 17\,600$

TABLE VII

Testing of Models for Complex Equilibria Using the SPEKTFOT Program in the Ga^{3+} System with Excess PANS

Model	GaL	GaL(OH)	GaL_2H	GaL_2
	log β ε, $mol^{-1}\,l.\,cm^{-1}$	log β ε, $mol^{-1}\,l.\,cm^{-1}$	log β ε, $mol^{-1}\,l.\,cm^{-1}$	log β ε, $mol^{-1}\,l.\,cm^{-1}$
Gal, Gal(OH), Ga(OH), $Ga(OH)_2$ $U = 6{\cdot}93\,.\,10^{-4}$; $\sigma(A) = 0{\cdot}006^a$ $U = 2{\cdot}90\,.\,10^{-3}$; $\sigma(A) = 0{\cdot}011^b$	$9{\cdot}87 \pm 0{\cdot}01^a$ $10{\cdot}04 \pm 0{\cdot}05^b$ $33\,185 \pm 273^a$ $34\,450 \pm 1\,480^b$	$6{\cdot}48 \pm 0{\cdot}11^a$ $3{\cdot}76 \pm 0{\cdot}03^b$ $27\,575 \pm 166^a$ $16\,630 \pm 10^b$	— — — —	— — — —
GaL, GaL_2H Ga(OH), $Ga(OH)_2$ $U = 1{\cdot}649\,.\,10^{-3}$; $\sigma(A) = 0{\cdot}009^a$ $U = 2{\cdot}901\,.'10^{-3}$; $\sigma(A) = 0{\cdot}013$	$9{\cdot}81 \pm 0{\cdot}02^a$ $10{\cdot}05 \pm 0{\cdot}013^b$ $33\,138 \pm 2\,160^a$ $34\,380 \pm 430^b$	—	$21{\cdot}33 \pm 0{\cdot}02^a$ $19{\cdot}66 \pm 1{\cdot}70^b$ $31\,368 \pm 400^a$ $40\,100 \pm 10\,000^b$	—
GaL, GaL_2 GaOH, $Ga(OH)_2$ $U = 2{\cdot}711\,.\,10^{-3}$ [a] $\sigma(A) = 0{\cdot}011$ $U = 2{\cdot}99\,.\,10^{-3}$ [b] $\sigma(A) = 0{\cdot}013$	$9{\cdot}96 \pm 0{\cdot}02^a$ $10{\cdot}05 \pm 0{\cdot}01^b$ $31\,300 \pm 240^a$ $34\,250 \pm 300^b$	—	—	$16{\cdot}04 \pm 0{\cdot}03^a$ $17{\cdot}29 \pm 1{\cdot}29^b$ $39\,158 \pm 883^a$ $38\,374 \pm 460^b$
GaL, GaL_2H, GaL_2 $U = 2{\cdot}078\,.\,10^{-3}$ [a] $\sigma(A) = \pm 0{\cdot}011$ Ga(OH), $Ga(OH)_2$	$9{\cdot}89 \pm 0{\cdot}02^a$ $30\,720 \pm 190^a$		$20{\cdot}81 \pm 0{\cdot}22^a$ $32\,080 \pm 120^a$	$16{\cdot}13 \pm 0{\cdot}36^a$ $37\,020 \pm 1\,050^a$

GaL, GaL(OH), GaL_2H	10·005 ±	0·065[a]	7·132 ±	0·075[a]	21·374 ±	0·029[a]
Ga(OH), $Ga(OH)_2$	10·110 ±	0·025[b]	6·96 ±	0·0045[b]	55 130 8 ±	4 600[a]
$U = 8{\cdot}329 \cdot 10^{-4}$ [a]	21 516 ±	232[a]	27 786 ±	172[a]	20·715 ±	0·0023[b]
$\sigma(A) = \pm 0{\cdot}009$[a]	28 660 ±	1[b]	28 353 ±	147[b]	97 730 ±	2[b](?)
$U = 2{\cdot}7183 \cdot 10^{-3}$ [b]						
$\sigma(A) = \pm 0{\cdot}013$[b]						

[a] $c_L = 3{\cdot}00 \cdot 10^{-4}$; [b] $4{\cdot}00 \cdot 10^{-4}$ M

Input data:

GaL (Ga + L ⇌ GaL); log $\beta = 9{\cdot}98$[c] $\varepsilon = 22\,200$[c]
GaL_2 (Ga + 2 L ⇌ GaL_2); log $\beta = 20{\cdot}00$ $\varepsilon = 45\,000$
GaL_2H (Ga + 2 L + H ⇌ GaL_2H); log $\beta = 15{\cdot}00$; $\varepsilon = 33\,000$
GaL(OH) (Ga + L + H_2O ⇌ GaL(OH) + H); log $*\beta = 7{\cdot}15$[c]; $\varepsilon = 28\,700$[c]
Ga(OH) (Ga + H_2O ⇌ GaOH + H); log $*\beta = -2{\cdot}87$
$Ga(OH)_2$ (Ga + 2 H_2O ⇌ $Ga(OH)_2$ + 2 H^+); log $*\beta = -6{\cdot}54$

Median optimized parameter values:

GaL (log $\beta = 10{\cdot}06 \pm 0{\cdot}06$; $\varepsilon = 2{\cdot}15 \cdot 10^4$ [d])
GaL_2H (log $\beta = 21{\cdot}05 \pm 0{\cdot}32$; $\varepsilon = 5{\cdot}5 \cdot 10^4$ [d])
GaL(OH) (log $*\beta_1 = 7{\cdot}05 \pm 0{\cdot}08$; $\varepsilon = 2{\cdot}8 \cdot 10^4$)
$Ga(OH)_2$ (log $*\beta_2 = -6{\cdot}56 \pm 0{\cdot}037$)
Ga(OH) (log $*\beta_1 = -3{\cdot}34 \pm 0{\cdot}017$)

[c] Values from graphical analysis of the absorbance curves; [d] from values for solutions with $c_L = 3{\cdot}00 \cdot 10^{-4}$ M alone.

of ε (GaL) do not correspond to the ε values obtained from graphical analysis nor to the ε values found for solutions with excess cation. The value of constant ε (GaL) also differs markedly for the two reagent concentrations. Model 2 (mixtures of GaL and GaL_2H in addition to hydrolysis of Ga^{3+}) and model 3 (mixtures of GaL and GaL_2) yield anomalously high values of ε for complex GaL and unusually small values of ε for the other complex, *e.g.* $\varepsilon(GaL_2)/\varepsilon(GaL) = 1{\cdot}25$, which is much less than the expected value of 2. Ternary model 3 (GaL, GaL_2H and GaL_2) gives stability constant values with relatively small standard deviations, but here also ε (GaL)/ $/\varepsilon(GaL_2) \ll 2$.

In indium solutions with excess 1-PAN-4S and with $c_M = 2{\cdot}0 \,.\, 10^{-5}$M and $c_L/c_M = 10$, the absorbance values were minimized in the range pH 1·50–3·80 (altogether 24 experimental points) unambiguously confirming the model with InL and InL_2, in good agreement with the results of graphical analysis. The optimum fit was obtained assuming that, under the experimental conditions, hydrolysis of In^{3+} to $In(OH)^{2+}$ and $In(OH)_2^+$ at pH 1·5–3·8 and for $c_M = 2{\cdot}0 \,.\, 10^{-5}$M does not have a marked effect on the complex equilibria (Table VIII). This is in agreement with the work of Biedermann[23], who found that $Z = [OH]_{bonded}/In^{3+} = 0{\cdot}5$ even for a hundred times higher concentration of indium ($c_M = 10^{-3}$M). In the presence of relatively stable complexes and for $c_M = 10^{-5}$, the concentration of hydrolyzed In^{3+} ions is negligible. Because minimization of the $\log {}^*\beta_1 = -3{\cdot}48$ and $\log {}^*\beta_2 = -7{\cdot}68$ values[16] for formation of the InOH and $In(OH)_2$ complexes also does not give a better fit, these constant values cannot be accurate. Compared with graphical analysis of the absorbance curves, minimization according to the SPEKTFOT program yields higher values of the molar absorption coefficients for complexes InL and InL_2 (Table VIII).

In thallium(III) solutions with excess ligand ($c_L/c_M = 9{\cdot}29$) minimization of absorbance data in the range pH −0·20 to 1·70 (altogether 20 experimental points)

TABLE VIII

Results of Minimization of Absorbance Data by the SPEKTFOT Program in the In^{3+}–1-PAN-4S System

$c_M = 1{\cdot}0 \,.\, 10^{-5}$M, $c_L/c_M = 10$, $= 540$ nm. Input data: InL: $\log \beta_1(In + L \rightleftharpoons InL) = 9{\cdot}92$; $\varepsilon = 25\,000$; InL_2: $\log \beta_2(In + 2\,L \rightleftharpoons InL_2) = 17{\cdot}74$; $\varepsilon = 34\,800$.

Complex	$\log \beta$	$\varepsilon \pm \Delta\varepsilon$	U	σ, A
InL	9·964 ± 0·006	28 963 ± 291	$1{\cdot}86 \,.\, 10^{-4}$	±0·003
InL_2	18·042 ± 0·018	44 414 ± 629		

also excluded the possibility of the presence of the TlL and TlL_2 chelates, where hydrolysis of Tl(III) to $TlOH^{2+}$ and $Tl(OH)_2^+$ (ref.[19]) does not play an important role. The increased value of the molar absorption coefficient for TlL_2 after minimization with the SPEKTFOT program compared to the results of graphical analysis indicates an incorrect extrapolation of transformations (*15*) and (*16*) or incomplete formation of chelate under optimum conditions. The minimization results are given in Table IX.

Using the HALTAFALL SPEFO (ref.[25]) program, the values found were used to construct distribution diagrams for all the components in the Ga–PANS, In–PANS and Tl(III)–PANS systems. For the Ga–PANS system, distribution diagrams confirm that GaL(LH) is formed only to a degree of 15–20% in solutions with $c_L = 3{\cdot}0 . 10^{-4}$M and $4{\cdot}0 . 10^{-4}$M at pH 3 and that at pH 3·5–8·0, GaL(OH) completely predominates. In solutions with excess cations ($c_M = 4 . 10^{-4}$M), 35% GaL(OH) is already formed in solutions with pH 2·5 (Fig. 9*a*); this is, however, not reflected in graphical analysis of the curves. Distribution diagrams for the In–PANS system (Fig. 10*b*) confirm that hydrolysis of In^{3+} to InOH and $In(OH)_2$ is almost negligible (the maximum content of InOH is at pH 2·4 (3·3%) and of $In(OH)_2$ at pH 7 (1%)). In solutions with excess cation higher ML_2 complexes are formed in indium systems similar to the Tl(III)–PANS system (Fig. 11*a*) (InL_2 at pH 5–30% and TlL_2 – 100%), with marked hydrolysis of M^{3+}. It also follows from the distribution diagrams

TABLE IX

Results of Minimization of the Absorbance Data by the SPEKTFOT Program in the Tl^{3+}–1-PAN-4S System

Input data: TlL: $\log \beta_1(Tl + L \rightleftharpoons TlL) = 14{\cdot}18$; $\varepsilon = 19\,460$; TlL_2: $\log \beta_2(Tl + 2\,L \rightleftharpoons TlL_2) = 26{\cdot}56$; $\varepsilon = 33\,500$; TlOH: $\log {}^*\beta_1(Tl + H_2O \rightleftharpoons TlOH + H) = -1{\cdot}18$ [ref.[16]]; $Tl(OH)_2$: $\log {}^*\beta_2(Tl + 2\,H_2O \rightleftharpoons Tl(OH)_2 + 2\,H^+) = -2{\cdot}73$ [ref.[16]]. $c_M = 2{\cdot}152 . 10^{-5}$M; $c_L/c_M = 9{\cdot}29$; $I = 0{\cdot}1$; 540 nm.

Complex	$\log \beta$	$\varepsilon \pm \Delta_\varepsilon$	U	σ, A
TlL	14·23 ± 0·03	19 997 ± 325	$1{\cdot}660 . 10^{-3}$	$0{\cdot}009_6$
TlL_2	26·62 ± 0·08	38 108 ± 385		
TlOH	−1·39 ± 0·28			
$Tl(OH)_2$	−2·93 ± 2·34			
TlL	14·23 ± 0·02	20 078 ± 272	$1{\cdot}607 . 10^{-3}$	0·009
TlL_2	26·61 ± 0·05	38 044 ± 523		
TlL	14·18 ± 0·05	20 425 ± 503	$1{\cdot}53 . 10^{-3}$	0·009
TlL_2	26·52 ± 0·10	38 189 ± 378		

that 100% formation of GaL(OH), InL_2 and TlL_2 occurs in solutions with excess reagent at pH 5·5, 6·0 and 2·5, respectively, before formation of strongly absorbing L^{2-} anions.

Spectrophotometric Determination of Gallium, Indium and Thallium with 1-PAN-4S

Optimum conditions for the determination of gallium are: pH 3·50–4·50, $c_L = 2{\cdot}0 \cdot 10^{-4}$M, $c_L/c_M \geqq 7$, $c_M \leqq 2{\cdot}8 \cdot 10^{-5}$M or 3·8 μg.ml^{-1}, 560 nm, acetate buffer (pH 4·48) ≦ 0·1M, in the presence of which the relative absorbance change compared with a pure solution is 0·1%. The following substances decreased the value of ε_k by 6–14% relative to ε_k for the pure solution in the presence of $c_L/c_M = 7{\cdot}5$: 0·1–0·05% polyvinyl alcohol, 0·01M sodium laurylsulphate, 0·5% solvasol 0 and $2 \cdot 10^{-5}$M antipyrine. The following substances do not interfere: Ca, Mg, Al (40 : 1), Mn(II) (10 : 1), acetate, As(III), As(V), Cl^-, Br^-, I^-, SO_4^{2-}, ClO_4^-, NO_3^- (1000 : 1). The following strongly interfere: Zr(IV), Hg(II), Ti(IV), Cr(III), Ni, Fe(II, III), In, Tl(III), Hf(IV),

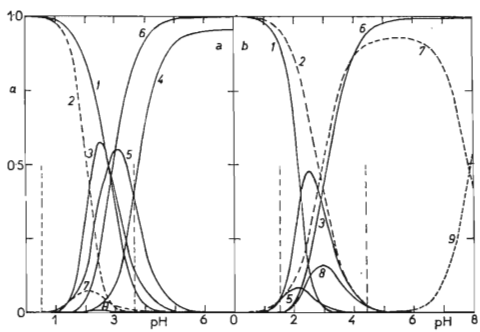

FIG. 9

Distribution Diagrams in the Ga–PANS System in Dependence on the pH

a) $c_L = 2{\cdot}00 \cdot 10^{-5}$M; $c_M = 4{\cdot}00 \cdot 10^{-4}$M, α for LH_2, LH and L and for the complexes was calculated with respect to the reagent; for M^{3+}, M(OH) and $M(OH)_2$ with respect to the metal. *1* Ga^{3+}, *2* LH_2, *3* GaL, *4* $Ga(OH)_2^+$, *5* $Ga(OH)^{2+}$, *6* GaL(OH), *7* LH^-, *8* GaL(LH). $C_{Ga} = 4{\cdot}00 \cdot 10^{-4}$M, $C_{LH_2} = 2{\cdot}00 \cdot 10^{-5}$M. *b*) $c_M = 2{\cdot}00 \cdot 10^{-5}$M, $c_L = 3{\cdot}00 \cdot 10^{-4}$M; α for M^{3+}, M(OH), $M(OH)_2$ and for the complexes calculated with respect to the metal, for LH_2, LH and L with respect to the concentration of reagent. The vertical dotted lines represent the border of the experimental region. *1* Ga^{3+}, *2* LH_2, *3* GaL, *5* $Ga(OH)^{3+}$, *6* GaL(OH), *7* LH^-, *8* GaL(LH), *9* L^{2-}.

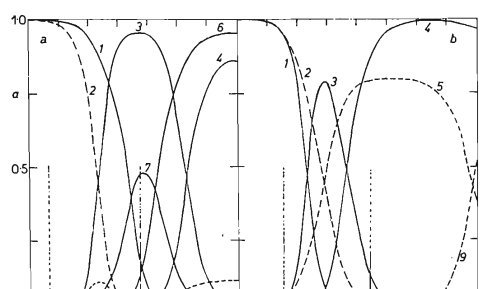

FIG. 10

Distribution Diagrams in the In–PANS System in Dependence on the pH

a) $c_M = 2{\cdot}0 \cdot 10^{-4}$M, $c_L = 2{\cdot}0 \cdot 10^{-5}$M; *1* In^{3+}, *2* LH_2, *3* In_2, *4* InL_2, *5* LH^-, *6* $In(OH)_2^+$, *7* $In(OH)_2^{2+}$. $C_{In} = 2{\cdot}00 \cdot 10^{-4}$M, $C_{LH_2} = 2{\cdot}00 \cdot 10^{-5}$M, *b*) $c_M = 2{\cdot}0 \cdot 10^{-5}$M, $c_L = 2{\cdot}0 \cdot 10^{-4}$M; α see Fig. 9. *1* In^{3+}, *2* LH_2, *3* In_2, *4* InL_2, *5* LH^-, *6* $In(OH)_2^+$, *7* $In(OH)_2^{2+}$. $C_{In} = 2{\cdot}00 \cdot 10^{-4}$M, $C_{LH_2} = 2{\cdot}00 \cdot 10^{-5}$M. *1* In^{3+}, *2* LH_2, *3* InL, *4* InL_2, *5* LH^-, *8* $In(OH)^{2+}$, *9* L^{2-}. $C_{In} = 2{\cdot}00 \cdot 10^{-5}$M, $C_{LH_2} = 2{\cdot}00 \cdot 10^{-4}$M.

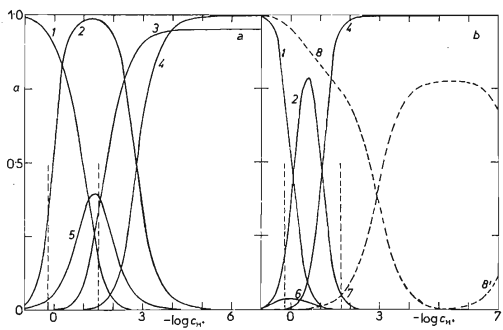

FIG. 11

Distribution Diagrams in the Tl(III)–PANS System in Dependence on the pH

a) $c_M = 4{\cdot}32 \cdot 10^{-4}$M, $c_L = 4{\cdot}00 \cdot 10^{-5}$M; *1* Tl^{3+}, *2* TlL^+, *3* $Tl(OH)_2^+$, *4* TlL_2^-, *5* $TlOH^{2+}$. $C_H = 4{\cdot}32 \cdot 10^{-4}$M, $C_L = 4{\cdot}00 \cdot 10^{-5}$M. *b*) $c_M = 2{\cdot}15 \cdot 10^{-5}$M, $c_L = 2{\cdot}00 \cdot 10^{-4}$M; α see Fig. 9. *1* Tl^{3+}, *2* TlL^+, *4* TlL_2^-, *6* $Tl(OH)^{2+}$, *7* LH^-, *8* LH_2, *8'* L^{2-}. $C_H = 2{\cdot}152 \cdot 10^{-5}$M, $C_L = 2{\cdot}00 \cdot 10^{-4}$M.

Bi(III), Pb(II), Zn, the lanthanoids, Cu, Sb(III) Zn, Y as well as SCN^-, phosphate, 1,10-phenanthroline, succinate, malonate, citrate, tartrate, oxalate, EDTA, CDTA, ascorbic acid, $S_2O_3^{2-}$, thiourea in ratios of 100 : 1. The interference limit corresponded to a $c_X : c_M$ ratio, where the relative absorbance change is $\pm 2\%$ compared to a pure solution. In^{3+} has a marked positive effect on the determination of gallium, leading to a shift and increasing the slope of the calibration curve from a ratio of $c_{In}/c_{Ga} = 0{\cdot}25$.

Optimum conditions for the determination of indium are: pH 3·50–4·50, $c_L = 2{\cdot}0 \cdot 10^{-4}$M, $c_L/c_M \geqq 7$, $c_M \leqq 2{\cdot}8 \cdot 10^{-5}$M or $\leqq 3{\cdot}22 \mu g.ml^{-1}$, 550–560 nm. All buffers suitable for this pH range interfere; 0·1M acetate buffer decreases the absorbance value by 12% relative. The following substances do not interfere: Ca, Mg, Al (40 : 1), Mn(II) (10 : 1), SO_4^{2-}, ClO_4^-, NO_3^-, As(III), As(V). The following interfere strongly: (1 : 1) SCN^-, Cl^-, Br^-, I^-, acetate, tartrate, citrate, malonate, succinate, oxalate, EDTA, CDTA, thiosulphate, thiourea, 1,10-phenanthroline, ascorbic acid, as well as (<5 : 1) Hg(II), Zr, Y, Sb(III), Cd, Cr(III), Cu, Ni, Ga, Fe(II, III), Tl(III), Hf, Bi, Pb, Zn, Cd, lanthanoids. Ga^{3+} interferes in the determination of indium from a ratio of $c_{Ga}/c_{In} = 0{\cdot}024$. In the presence of gallium the calibration curve for indium is shifted to higher absorbance values. At higher concentrations of the determined element, the calibration curves for gallium or indium in the presence of the other element are concavely deformed, possibly as a result of lack of reagent in the solution for both the determined and interfering component; formation of the ternary $InGaL_x$ complex in the presence of small indium concentrations is also a possible factor. The selectivity coefficients k_p and k_a (ref.[17]) were calculated for selected concentrations of the determined element according to relationships (*25*) and (*26*):

$$k_p = \frac{(A_f - A_0)\, c_d}{(A_d - A_0)\, c_f}, \qquad (25)$$

$$k_a = \frac{(A_{df} - A_d) - (A_f - A_0)}{(A_d - A_0)\, c_f}, \qquad (26)$$

where A_0 is the absorbance of the blank, A_d is the absorbance of the pure solution of the analyzed component with concentration c_d, A_f is the absorbance of the interfering substance with concentration c_f (for $c_d = 0$) and A_{df} is the absorbance of the solution containing both c_d and c_f.

For determination of gallium ($c_d = 2 \cdot 10^{-6} - 1{\cdot}6 \cdot 10^{-5}$M) the selectivity coefficients of indium are: $k_p = 1{\cdot}23$; 1·24 and $k_a = 5 \cdot 10^4$; $4 \cdot 10^4$ ($c_f = 4 \cdot 10^{-6}$M, or $8 \cdot 10^{-6}$M respectively). For the determination of indium ($c_d = 2 \cdot 10^{-6} - 1{\cdot}6 \cdot 10^{-5}$M) the selectivity coefficients of gallium are: $k_p = 0{\cdot}72$; 0·78 and $k_a = 3 \cdot 10^4$ $2 \cdot 10^4$ ($c_f = 4 \cdot 10^{-6}$M or $8 \cdot 10^{-6}$M respectively).

In the determination of gallium and indium, interfering thallium can be reduced with HSO_3^- from a concentration of 10^{-3}M-HSO_3^- in acidic media and excess reducing agent is removed by boiling. Thallium(I) does not interfere.

Optimum conditions for the determination of thallium are: pH 2·00, $c_L = 4{\cdot}0 \,.\, 10^{-4}$M, $c_M \leqq 1 \,.\, 10^{-5}$M or $\leqq 4$ μg. ml^{-1}, $c_L/c_M \geqq 7$, 560–570 nm. 0·1M glycolate buffer decreases the absorbance by 7·6% relative to a pure solution, other buffers suitable for this pH region interfere. The following substances also interfere: reducing agents, SCN^-, Cl^-, Br^-, I^-, $S_2O_3^{2-}$, succinate, tartrate, malonate, citrate, oxalate, EDTA, CDTA, and the following strongly interfere: Ni, Cu, Fe(II, III), Hg(II), Bi, Ga, In, Sc, Y, La, lanthanoids. The following do not interfere: Ca, Mg, Mn(II), Pb, Al(250 : 1), Cr(III), Cd(80 : 1), Zn(20 : 1). Traces of Cl^- and Br^- produce a decrease in the slope of the calibration curve for Tl(III) and concave bending of the curve for small concentrations of Tl(III). Some characteristics of the methods for the determination of gallium, indium and thallium are given in Table X.

TABLE X

Some Characteristics of the Spectrophotometric Determination of Gallium, Indium, Thallium with 1-PAN-4S Calculated from the Calibration Curves by the STAT Program (ref.[22])

Conditions	s_{xy} (A)	s_{xy} (c) μg . ml^{-1}	Blank absorb. Δ	s_B	$\varepsilon \pm \Delta\varepsilon$ mol^{-1} l . cm^{-1}	Detection limit μg . ml^{-1} [a]	λ_{nm}
			Ga				
$c_L = 2{\cdot}0 \,.\, 10^{-4}$M	$3{\cdot}73 \,.\, 10^{-3}$	$1{\cdot}08 \,.\, 10^{-2}$	0·392	0·002	23 938 ± 102	0·046	550
pH 3·50	$2{\cdot}14 \,.\, 10^{-3}$	$6{\cdot}36 \,.\, 10^{-3}$	0·209	0·001	23 433 ± 58	0·027	560
pH 4·50	$4{\cdot}96 \,.\, 10^{-3}$	$1{\cdot}47 \,.\, 10^{-2}$	0·421	0·002	23 516 ± 135	0·062	550
	$2{\cdot}69 \,.\, 10^{-3}$	$8{\cdot}17 \,.\, 10^{-3}$	0·228	0·001	22 969 ± 80	0·035	560
			In				
$c_L = 4{\cdot}0 \,.\, 10^{-4}$M	$2{\cdot}57 \,.\, 10^{-3}$	$1{\cdot}06 \,.\, 10^{-2}$	0·398	0·001	27 902 ± 76	0·045	550
pH 3·50	$3{\cdot}60 \,.\, 10^{-3}$	$1{\cdot}49 \,.\, 10^{-2}$	0·208	0·002	27 762 ± 98	0·063	560
pH 4·50	$4{\cdot}10 \,.\, 10^{-3}$	$1{\cdot}53 \,.\, 10^{-2}$	0·419	0·002	30 711 ± 112	0·065	550
	$4{\cdot}11 \,.\, 10^{-3}$	$1{\cdot}56 \,.\, 10^{-2}$	0·226	0·002	30 265 ± 112	0·066	560
			Tl				
c_L M $4 \,.\, 10^{-4}$M pH 4·50	$5{\cdot}83 \,.\, 10^{-3}$	$3{\cdot}41 \,.\, 10^{-2}$	0·151	0·002	34 953 ± 166	0·145	560

[a] $3S_{xy}\sqrt{2}$.

The absorption coefficients for the Ga–PANS, In–PANS and Tl(III)–PANS systems calculated by the minimization procedure using the SPEKTFOT program generally have higher values, especially for the InL_2 complex at 540 nm than the values calculated from the plateau of the absorbance – pH curves, from the limit of the graphical transformations and from the slopes of the calibration curves. For example, the molar absorption coefficients for 540 nm for InL_2 are $\varepsilon = 3{\cdot}50 \cdot 10^4$ (graphical analysis) and $4{\cdot}44 \cdot 10^4$ (calculated by the SPEKTFOT program), and for TlL_2 $\varepsilon = 3{\cdot}40 \cdot 10^4$ (graphical analysis) and $3{\cdot}80 \cdot 10^4$ (calculated). Consequently, under optimum conditions, *e.g.* on the horizontal branch of the absorbance *vs* pH curve for solutions with excess reagent, the particular complex is not formed quantitatively, but rather in a mixture with previous complexes in the series which absorb less or with partial hydrolysis. Thus in such cases the horizontal branch of the absorbance curve need not indicate quantitative formation of a single complex.

It follows from the distribution diagrams (Fig. 10, 11) that, *e.g.* only 75% of the indium present at pH 4 is in the form of InL_2 and that at pH 1·5 only 88% of the thallium present is in the form of TlL_2, *i.e.* under conditions prescribed for the spectrophotometric determination of these elements with 1-PANS. The remainder is in the form of the lower 1 : 1 complex which absorbs less. From a practical point of view the constant value of the absorbance from pH 3·5–4·0 for gallium and indium and from pH 1·5 for thallium permits spectrophotometric determination of these elements at a lower pH value than indicated by distribution diagrams.

REFERENCES

1. Langová M., Sommer L.: Folia Fac. Sci. Nat. Univ. J. E. Purkyně Brno, Vol. 9, Chemia 6, Part *2* (1968).
2. Shibata Sh. in the book: *Chelates in Analytical Chemistry* (H. A. Flaschka, A. J. Barnard, jr, Eds), Vol. 4. Dekker, New York 1973.
3. Hovind H. R.: Analyst (London) *100*, 769 (1975).
4. Sommer L., Koblížková V.: This Journal *39*, 369 (1974).
5. Koblížková V., Kubáň V., Sommer L.: This Journal *43*, 2711 (1978).
6. Koblížková V., Kubáň V., Sommer L.: Chem. Zvesti, in press.
7. Kubáň V., Havel V., Sommer L.: This Journal *30*, 604 (1975).
8. Kubáň V., Havel J.: Proposed Improvement ZN 13/76, UJEP Brno.
9. Havel J.: Chem. Listy *62*, 1250 (1968).
10. Sommer L., Kubáň V., Havel J.: Folia Fac. Sci. Nat. Univ. J. E. Purkyně Brno, Vol. 11, Chemia 7, Part *1* (1970).
11. Havel J., Kubáň V.: Scripta Fac. Sci. Nat. Univ. J. E. Purkyně Brno, Chemia 2, *1*, 87 (1971).
12. Kubáň V.: Scripta Fac. Sci. Nat. Univ. J. E. Purkyně Brno, Chemia 2, *2*, 81 (1972).
13. Vošta J., Havel J.: Report, Department of Analytical Chemistry, Univ. Brno 1974, Part II.
14. Suchánek M.: *Thesis*. Prague Institute of Chemical Technology, Prague 1976.
15. Sommer L., Havel J.: This Journal *42*, 2134 (1977).
16. Nazarenko V. V., Biryuk E. A., Ravitskaya R. V.: Zh. Anal. Khim. *30*, 74 (1975).

17. Klika Z., Sommer L.: Scripta Fac. Sci. Nat. Univ. J. E. Purkyně Brno, Chemia 2, *8*, 53 (1978).
18. Havel J.: Unpublished results.
19. Biedermann G.: Arkiv Kemi *5*, No *41*, 441 (1953).
20. Busev A. I., Tiptsova V. G.: Zh. Anal. Khim. *13*, 180 (1958).
21. Doležal J., Šír Z., Janáček K.: This Journal *21*, 1300 (1956).
22. Sommer L., Langová M., Kubáň V.: Scripta Fac. Sci. Nat. Univ. J. E. Purkyně Brno, Chemia 1, *8*, 13 (1978).
23. Biedermann G.: Arkiv Kemi *9*, 277 (1956).
24. Havel J., Rabová D., Sommer L.: Scripta Fac. Sci. Nat. Univ. J. E. Purkyně Brno, Chemia 3, *7*, 101 (1977).
25. Havel J., Pavlíková N.: Scripta Fac. Sci. Nat. Univ. J. E. Purkyně Brno, in press.

Translated by M. Štuliková.